Thermodynamics of copper sulfides

I. Heat capacity and thermodynamic properties of copper(I) sulfide, Cu₂S, from 5 to 950 K [a]

FREDRIK GRØNVOLD

Department of Chemistry, University of Oslo, Blindern, 0315 Oslo 3, Norway

and EDGAR F. WESTRUM, JR.

Department of Chemistry, University of Michigan, Ann Arbor, Michigan 48109, U.S.A.

The heat capacity of Cu_2S from 5 to 950 K was determined by adiabatic-shield calorimetry and the thermodynamic properties were evaluated. Transitions occur at 376 and about 710 K with $\Delta_{trs}S_m = (1.240 \pm 0.006)R$ and $(0.201 \pm 0.006)R$. Considerable hysteresis was involved in achieving equilibrium in the latter transition. At 298.15 and 950 K the values of $C_{p,m}(T)$, $S_m^\circ(T)$, and $\Phi_m^\circ(T, 0)$ are 9.242R, 13.987R, and 7.6121R; and 9.960R, 27.810R, and 17.875R, respectively. Subtraction of the estimated lattice heat capacity at constant pressure leaves a large excess heat capacity, especially for the fast ionic conductor β-Cu_2S. It is about 2.8R at 400 K and decreases gradually to 1.26R at 680 K. Its origin is discussed.

1. Introduction

In this series the thermodynamic properties of copper sulfides will be treated on the basis of existing thermophysical and formation properties and heat capacities obtained by us for different Cu_xS samples ($x = 1.00$, 1.75, 1.80, 1.85, 1.90, 1.95, 1.98, 1.995, and 2.00), several of them over the range 5 to about 1000 K. The need for studying a large number of samples arises from the complexity of the system. In earlier days it was assumed to be simple, having only two solid phases, CuS and Cu_2S, but now the region $Cu_{1.75}S$ to $Cu_{2.00}S$ presents a bewildering array of more than 10 crystallographically characterized species. Among these are: anilite ($Cu_{\approx 1.75}S$), five modifications of digenite ($Cu_{\approx 1.80}S$), djurleite ($Cu_{\approx 1.95}S$), and three stable and one metastable modification of chalcocite (Cu_2S). The present paper (Part I) concerns the heat capacity of copper(I) sulfide, Cu_2S, and the derived thermodynamic properties.

The low-temperature heat capacity of Cu_2S was determined by Anderson[1] over the region 53 to 293 K and a standard molar entropy at 298.15 K was derived. A variety of slightly differing values has been obtained from equilibrium studies (see Mills[2] and Potter[3]). In view of the considerable breadth of the low-end extrapolation by Anderson, a redetermination of the low-temperature heat capacity of Cu_2S was deemed necessary. During the course of this investigation, Ferrante et al.[4] have presented heat-capacity results for Cu_2S from 5 to 310 K and enthalpy results from 298 to 1600 K by drop calorimetry.

Above 300 K the heat-capacity behavior of Cu_2S is profoundly influenced by the crystallographic changes occurring near 375 and 710 K. According to Evans,[5] the structure of γ-Cu_2S (low-chalcocite) is monoclinic—not orthorhombic as earlier reported[6-12]—and gives no evidence of positional disorder or partially filled sites. The structure of the intermediate phase, β-Cu_2S (high-chalcocite), is hexagonal[9,11-16] with the S atoms arranged in a nearly perfect close-packing and the Cu atoms distributed in the interstices in an almost fluid-like way.[14-16] On further increase in temperature α-Cu_2S (high-chalcocite) or high-digenite) is formed. Its structure is face-centered cubic[7,11,17,18] and is assumed[17] to be of the anti-fluorite type.

Early enthalpy-increment[19-21] and heat-capacity[11,22] studies gave approximate values for the transitional enthalpies, but failed to reveal the gradually decreasing heat capacity of the intermediate β-Cu_2S phase with increasing temperature. Then, Jost and Kubaschewski[23] and Kubaschewski[24] found that the molar heat capacity of the β-form decreases over its entire range of existence, from $11.97R$ at 383 K to $10.80R$ at 673 K according to the later publication. At (708 ± 7) K, the heat capacity increases rapidly due to the transformation of β-Cu_2S(hex) into α-Cu_2S(cub). A constant molar heat capacity of $9.93R$ was found for α-Cu_2S up to 823 K, the highest temperature of the experiments. Several explanations of the anomalous heat-capacity behavior were suggested, but no definite conclusion was reached.

A decrease in heat capacity with increasing temperature over relatively wide temperature ranges can arise from a changing unpaired-electron distribution. This has often been observed for transition-metal compounds in the low-temperature range. Similar decreases also have been observed recently for some 3d-transition-element chalcogenides[25,26] above room temperature, where the electronic contribution to heat capacity is small compared with that of the lattice, and precise heat-capacity determinations are necessary to delineate the behavior of the heat-capacity curve. The partly non-cooperative magnetic type of transitions differs thermally from the structural order–disorder transitions in that the heat-capacity contribution on the high-temperature side usually decreases less abruptly than it does for the structural ones. This is, however, not always so, and interesting exceptions are found among copper and silver chalcogenides and halides.[27-29]

A thermodynamically consistent description of structural phase transitions based on the assumption that defect formation and entropy are unique functions of the molar volume of the crystal has been given by Schmalzried.[30]

Since all the earlier heat-capacity determinations had been carried out by continuous heating of the sample, we decided to reinvestigate copper(I) sulfide by

intermittently energized calorimeters with adiabatic shields. In this way more reliable values of the heat capacity and its temperature dependence could be obtained. Furthermore, it seemed of interest to consider the results in the light of available information about the structural changes of Cu_2S with temperature and lattice heat-capacity estimates.

2. Experimental

The copper(I) sulfide was prepared directly from the elements. The copper was in the form of a continuous cast rod, >99.999 mass per cent pure, from the American Smelting and Refining Co., New Jersey. The sulfur was 99.9999 mass per cent pure crystals from Koch-Light Laboratories, Colnbrook, England. Appropriate amounts of the elements were heated in an evacuated and sealed vitreous silica tube, constricted at the middle by a smaller-diameter tube. Copper was placed in one part of the tube and sulfur in the other, and the tube was put into a reclining tube furnace with the sulfur-containing compartment protruding. The copper was heated to 620 K and the sulfur was allowed to melt and flow into the hotter part of the tube. When most of the sulfur had combined with the copper, a heating pad was wound around the exterior end of the silica tube so that the remaining sulfur was brought into reaction. This was accomplished overnight. The empty half of the silica tube was sealed off and discarded before the sample was tempered at 670 K for 24 h. The sample was then finely crushed and transferred to the calorimetric ampoule.

X-ray powder photographs of the copper(I) sulfide were taken in Guinier-type cameras of 8.0 cm diameter. $Cu(K\alpha_1)$ radiation was used with KCl as a calibration substance $\{a(293 \text{ K}) = 629.19 \text{ pm}\}$.[31] The lattice constants of the orthorhombic subcell are: $a = (1188.5 \pm 0.4)$ pm, $b = (2732.2 \pm 1.3)$ pm, $c = (1349.6 \pm 0.4)$ pm. They agree well with the results by Djurle:[12] $\{a = (1188.1 \pm 0.4)$ pm, $b = (2732.3 \pm 0.8)$ pm, $c = 1349.1 \pm 0.4)$ pm$\}$ and by Potter and Evans:[32] $\{a = (1188.5 \pm 0.2)$ pm, $b = (2732.5 \pm 0.4)$ pm, $c = (1349.6 \pm 0.2)$ pm$\}$.

CALORIMETRY

5 *to* 350 K, *University of Michigan*. The Mark II cryostat and adiabatic method employed have been described elsewhere.[33] A gold-plated copper calorimeter (W-52) with a volume of 59 cm³ was used. The calorimeter was loaded with sample and evacuated, and helium gas to improve thermal equilibrium was added to 4.0 kPa pressure at about 300 K to provide thermal contact between sample and calorimeter. It was then sealed, placed in the cryostat, and cooled. The mass of sample used was 160.52 g. The calorimeter was surrounded by a shield system provided with automatic temperature control. Temperatures were measured with a capsule-type platinum resistance thermometer (A-5) located in a central well in the calorimeter. The heat capacity of the empty calorimeter determined in a separate set of experiments, amounted to 2 per cent at 5 K, 13 per cent at 50 K, and about 17 per cent above 100 K.

300 *to* 950 K, *University of Oslo.* The calorimetric apparatus and measuring technique have been described in detail[34] along with results obtained for the heat capacity of a standard sample of α-Al_2O_3. The calorimeter was operated with adiabatic shields and intermittent energy inputs with temperature equilibration between each input. The 50 cm^3 sample container of fused silica had a well for the heater and platinum resistance thermometer, axially located in the cylindrical silver calorimeter. The calorimeter-sample assembly was suspended inside a double-walled silver shield system with enclosed heaters. Outside the shields was a heated guard system, also of silver. The whole assembly was placed in a vertical tube furnace. The mass of sample used was 163.49 g. Heat-capacity measurements on the empty calorimeter were carried out in a separate series of experiments. They represent from 47 to 56 per cent of the total outside the transition regions. Small corrections were applied for differences in mass of the empty and full silica container and for "zero" drift of the calorimeter.

Calibrations and adjustments. The platinum resistance thermometer for the low-temperature calorimeter had been calibrated by the U.S. National Bureau of Standards—and that for the high-temperature calorimeter locally—at the ice, steam, and zinc points. Temperatures are judged to correspond to IPTS–68 within 0.02 K to 350 K and within 0.08 K above this temperature. Precision was considerably better and the temperature increments are probably accurate to 0.0002 K for the low-temperature region and to 0.002 K for the high-temperature region. Measurements of mass, resistance, potential difference, and time are referred to standardizations and calibrations performed at the U.S. National Bureau of Standards.

3. Results and discussion

HEAT CAPACITY AND THERMODYNAMIC PROPERTIES

The measured heat capacities of copper(I) sulfide from both low- and high-temperature ranges are listed in chronological order in table 1 and presented graphically in figure 1. The approximate temperature increments used in the determinations can usually be inferred from the adjacent mean temperatures in table 1.

Twice the standard deviation in the measured low-temperature heat capacity is about 1 per cent from 8 to 30 K, 0.1 per cent from 30 to 300 K, and 0.2 per cent from 300 to 350 K. In the higher-temperature region it is about 0.3 per cent. Below 10 K, the heat capacity was extrapolated with a $C_{p,\,m}/T$ against T^2 plot ($\gamma = 0$).

The low-temperature values of this research are in reasonable accord over the common range of measurement (53 to 293 K) with the earlier work of Anderson.[1] However, such differences as exist between their derived standard molar entropy $S_m^\circ(298.15 \text{ K}) = (14.54 \pm 0.25)R$ and ours $(13.987 \pm 0.024)R$ are primarily caused by errors in their extrapolation below 53 K. The value by Ferrante *et al.*[4] $S_m^\circ(298.15 \text{ K}) = 13.970R$ is practically equal to ours.

In agreement with earlier findings, we observed that the compound undergoes two transitions. One has a maximum molar heat capacity of $121.2R$ over a 1.46 K

TABLE 1. Heat capacity of copper(I) sulfide, Cu_2S ($R = 8.3144$ J·K⁻¹·mol⁻¹)

$M(Cu_2S) = 159.15$ g·mol⁻¹

High-temperature measurements—University of Oslo

⟨T⟩/K	$C_{p,m}/R$	⟨T⟩/K	$C_{p,m}/R$	⟨T⟩/K	$C_{p,m}/R$	⟨T⟩/K	$C_{p,m}/R$	⟨T⟩/K	$C_{p,m}/R$	⟨T⟩/K	$C_{p,m}/R$
Series I		532.01	11.344	769.50	10.043	470.03	11.586	391.72	11.937	832.73	9.929
328.67	9.659	542.15	11.295			479.81	11.557			841.71	9.925
338.98	9.815	552.92	11.234	Series V		489.64	11.529	Series IX			
349.18	10.091			575.02	11.173	499.54	11.474	663.14	10.910	Series XI	
$\Delta_{trs}H$ Detn. A		Series III		585.43	11.146	509.51	11.419	674.12	10.833	851.70	9.925
386.36	11.953	648.32	10.946	595.91	11.107	519.54	11.383	685.17	10.802	862.50	9.917
395.68	11.900	659.18	10.928	606.46	10.090			696.29	10.772	873.33	9.918
405.04	11.882	670.12	10.896	617.06	11.060	Series VII		$\Delta_{trs}H$ Detn. F		884.26	9.914
414.45	11.826	681.12	10.881	627.74	11.036	$\Delta_{trs}H$ Detn. D		747.17	83.61	895.27	9.896
423.90	11.788	$\Delta_{trs}H$ Detn. B		638.48	10.985					906.36	9.915
433.40	11.768	742.04	10.145	649.29	10.935	Series VIII		Series X		917.49	9.942
442.96	11.706	753.84	10.063	660.18	10.906	297.49	9.251	773.95	9.989	928.67	9.950
				671.15	10.884	304.71	9.320	782.50	9.973	938.93	9.967
Series II		Series IV		682.20	10.831	315.12	9.422	790.62	9.952	947.84	9.938
501.38	11.445	$\Delta_{trs}H$ Detn. C				325.46	9.583	799.03	9.962		
511.90	11.409	734.14	10.157	Series VI		335.74	9.707	807.39	9.923		
521.93	11.399	742.90	10.141	450.64	11.653	345.96	9.867	815.64	9.938		
		755.65	10.085	460.31	11.606	$\Delta_{trs}H$ Detn. E		824.01	9.954		

Low-temperature measurements—University of Michigan

⟨T⟩/K	$C_{p,m}/R$	⟨T⟩/K	$C_{p,m}/R$	⟨T⟩/K	$C_{p,m}/R$	⟨T⟩/K	$C_{p,m}/R$	⟨T⟩/K	$C_{p,m}/R$	⟨T⟩/K	$C_{p,m}/R$
Series I		16.45	0.6138	47.03	3.289	99.24	5.940	173.54	7.784	Series IV	
4.97	0.0242	18.07	0.7545	52.27	3.651	108.61	6.260	182.18	7.933	257.15	8.822
5.57	0.0268	19.78	0.9009	57.09	3.957	117.54	6.533	192.84	8.069	266.67	8.922
6.38	0.0381	21.43	1.0613	62.76	4.300	126.59	6.783	202.36	8.210	276.17	9.019
7.28	0.0616	22.80	1.1908			136.37	7.040	211.81	8.330	285.67	9.147
8.30	0.0948	24.60	1.3630	Series II		146.76	7.273	221.26	8.449	295.18	9.215
9.17	0.1235	27.07	1.5973	55.96	3.885	157.04	7.487	230.71	8.550	304.69	9.315
10.06	0.1711	29.64	1.8402	61.69	4.238			240.05	8.650	314.20	9.427
11.15	0.2286	32.48	2.1059	68.46	4.610	Series III		249.42	8.756	323.72	9.532
12.31	0.2996	35.50	2.377	75.57	4.960	144.75	7.228	258.96	8.856	333.15	9.647
13.55	0.3878	39.23	2.692	82.22	5.279	154.20	7.422	268.59	8.946	340.77	9.733
14.93	0.4935	42.99	2.986	89.93	5.607	163.89	7.615			347.55	9.866

interval around 374.6 K, and the other has a maximum of about 24.0R around 715 K. The approach to equilibrium is especially slow for the latter transition, and considerably higher heat-capacity values might obtain under conditions even closer to equilibrium. In the region between the transitions the heat capacity decreases considerably with increasing temperature, while above the β-Cu_2S-to-α-Cu_2S transition the heat capacity first decreases and then increases slightly again.

To evaluate and compare the different determinations through the transition regions, reference non-transitional heat-capacity curves have been estimated. For the low-temperature phase, γ-Cu_2S, the "non-transitional" molar heat capacity is assumed to increase linearly from 9.26R at 300 K to 9.98R at 375 K. For β-Cu_2S and α-Cu_2S, reference backgrounds were established by least-squares-fitted polynomial expressions for the heat capacity in the regions 386 to 682 K and 734 to 956 K, respectively. The curves were extrapolated to the transition temperatures, which for this purpose were taken to be 376 K for the $\gamma \rightarrow \beta$ transition and 710 K
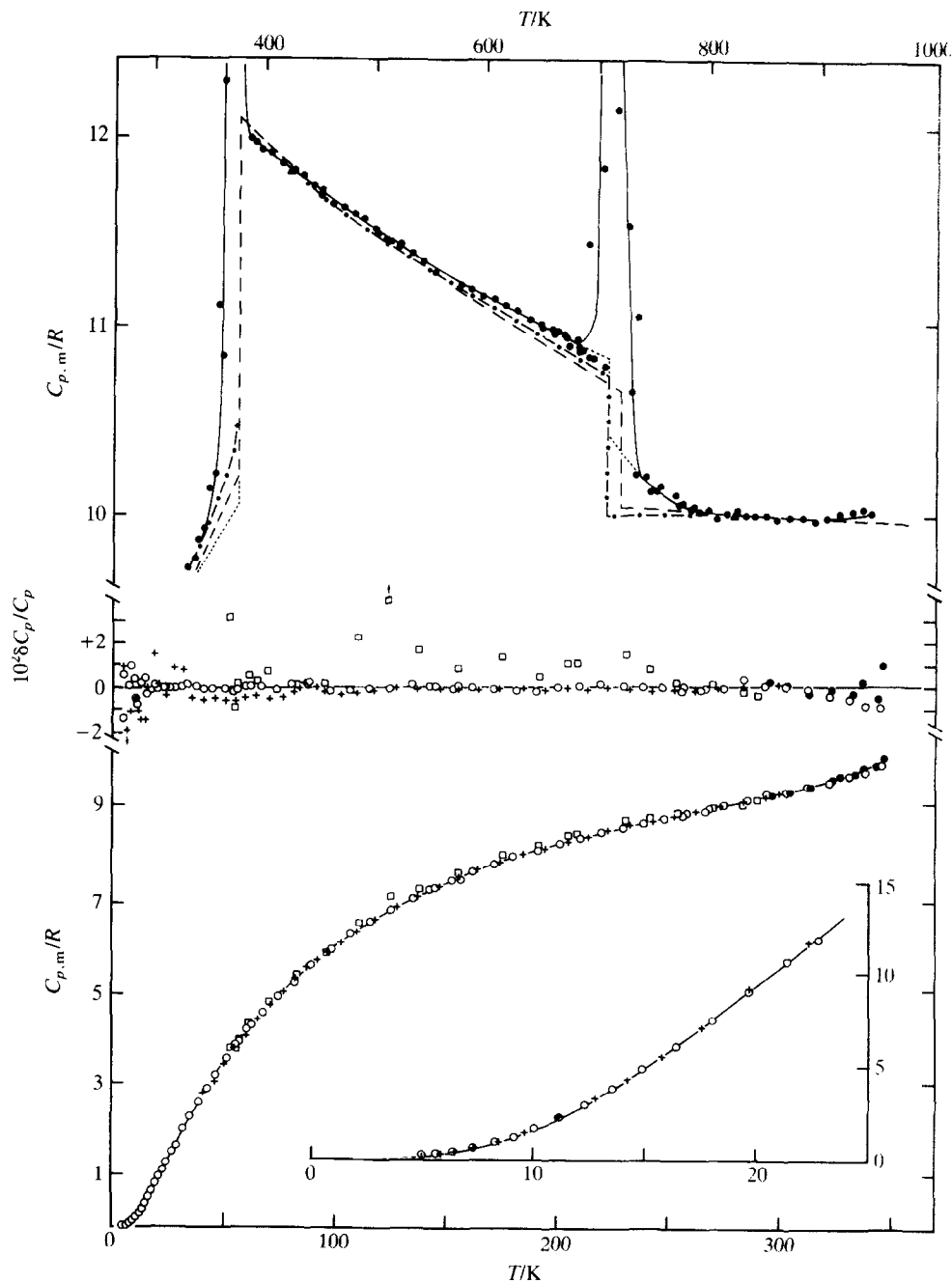
FIGURE 1. The molar heat capacity of Cu_2S. $\bigcirc$, The present low-temperature results; $\bullet$, the high-temperature results; $+$ or $- - -$, Ferrante et al.,[4] $\square$, the low-temperature results of Anderson;[1] $- \cdot -$, the results of Kubaschewski.[24] The deviations of the values of Anderson[1] and those of Ferrante et al.[4] from the present ones are shown in the center of the figure.

for the $\beta \to \alpha$ transition. The resulting molar heat capacities are $11.991R$ and $10.768R$, respectively.

Results of the transformation evaluations are given in table 2. The mean standard molar entropy for three determinations through the $\gamma \to \beta$ transition region is $\Delta_{trs}S_m^\circ = (1.240 \pm 0.006)R$. Pre- and post-transitional contributions from 300 to 390 K are included in these values. The equilibration time after the energy inputs varied from 41 to 83 min with no signs of delayed energy absorption. The results show more than usual spread, however, for such favorable equilibration conditions. Previous thermal history is possibly of importance, and uncertainty in the state of

TABLE 2. Evaluation of transitions in copper(I) sulfide ($R = 8.3144$ J $\cdot$ K^{-1} $\cdot$ mol^{-1})

$\langle T \rangle$	$C_{p,m}$	ΔT	$\Delta_{eq}t^a$	ΔH_m°	$\Delta_{nt}H_m^\circ{}^b$	$\Delta_{trs}H_m^\circ$	$\langle T \rangle$	$C_{p,m}$	ΔT	$\Delta_{eq}t^a$	ΔH_m°	$\Delta_{nt}H_m^\circ{}^b$	$\Delta_{trs}H_m^\circ$
K	R	K	min	$R \cdot$K	$R \cdot$K	$R \cdot$K	K	R	K	min	$R \cdot$K	$R \cdot$K	$R \cdot$K

$M(Cu_2S) = 159.15$ g $\cdot$ mol^{-1}

Transition: γ-Cu$_2$S to β-Cu$_2$S

$\Delta_{trs}H$ Detn. A							374.95	71.299	2.679	55	193.15	27.33	165.74
359.06	11.106	9.623	53	106.87	94.58	12.29	379.01	26.688	5.410	48	144.28	64.80	79.48
367.19	19.936	6.649	83	132.55	65.87	66.68	$\Delta_{300.00 K}^{354.25 K}H_m^\circ/(R \cdot$K):						6.15
372.06	53.151	3.076	75	163.49	30.62	132.87							463.28

$\Delta_{trs}H$ Detn. D							375.29	113.450	0.778	66	88.27	7.77	84.11
362.08	10.790	9.774	64	105.46	96.35	9.10	376.27	71.534	1.186	66	84.84	13.57	71.27
368.97	15.133	3.990	41	60.38	39.59	20.78	377.74	45.483	1.759	66	80.01	21.08	58.92
372.03	35.463	2.151	47	76.22	21.41	54.81	380.84	12.831	4.440	66	56.97	53.16	3.81
373.63	82.809	1.037	79	85.88	10.34	75.53	385.36	12.173	5.587	66	68.01	66.78	1.24
374.53	117.556	0.752	66	88.40	7.51	80.90	$\Delta_{300.00 K}^{357.20 K}H_m^\circ/(R \cdot$K):						7.48
													464.35

$\Delta_{trs}H$ Detn. E							374.62	121.210	1.465	67	177.57	14.63	162.95
356.10	10.165	10.087	59	102.54	98.86	3.68	376.80	58.794	2.879	59	169.27	33.24	136.03
365.69	12.262	9.089	59	111.44	89.92	21.53	382.64	13.023	8.822	59	114.89	105.55	9.33
372.07	43.342	3.654	74	153.38	36.37	122.01	$\Delta_{300.00 K}^{351.06 K}H_m^\circ/(R \cdot$K):						4.99
													460.51

$\langle \Delta_\gamma^\beta H_m^\circ \rangle = (462.7 \pm 2.2)R \cdot$K $\langle \Delta_\gamma^\beta S_m^\circ \rangle = (1.240 \pm 0.006)R$.

Transition β-Cu$_2$S to α-Cu$_2$S

$\Delta_{trs}H$ Detn. B							710.14	18.318	8.078	106	147.97	85.21	62.76
692.05	11.38	10.821	111	123.18	117.13	6.05	719.48	12.102	10.591	75	128.18	108.90	19.28
701.78	16.910	8.643	1135	146.16	93.30	52.86	730.48	10.61	11.403	75	120.96	116.33	4.63
													145.58

$\Delta_{trs}H$ Detn. C							718.84	13.402	5.052	382	67.70	51.97	15.73
705.82	11.792	5.333	35	62.89	57.43	5.46	723.48	18.505	4.247	1017	78.59	43.54	35.05
710.64	17.173	4.323	235	74.23	45.38	28.85	728.42	11.474	5.619	198	64.47	57.41	7.06
714.56	24.511	3.506	1118	85.94	36.19	49.75							141.90

$\Delta_{trs}H$ Detn. F							725.34	15.697	9.182	65	147.85	94.02	53.83
707.23	10.609	10.728	87	125.43	114.64	10.79	735.58	10.995	11.280	48	122.67	114.70	7.96
716.68	18.792	8.167	68	152.49	84.16	68.34							140.92

$\langle \Delta_\beta^\alpha H_m^\circ \rangle = (142.0 \pm 3.0)R \cdot$K $\langle \Delta_\beta^\alpha S_m^\circ \rangle = (0.201 \pm 0.006)R$.

^{a} $_{.q}$, Equilibration time. ^{b} $_{nt}$, Non-transitional.

definition might arise as a consequence of cooling the sample through the $\beta \to \alpha$ transition region.

The numerical results on the $\gamma \to \beta$ and $\beta \to \alpha$ transition enthalpies for copper(I) sulfide are summarized in table 3 and compared there with previous (and subsequent) determinations. The several studies of the $\gamma \to \beta$ transition over the past two decades are in reasonable accord. A perfect agreement exists with the old result by Bellati and Lussana,[19] while the results by Ueda,[11] Kubaschewski,[24] and Ferrante et al.[4] are somewhat lower, and the result by Hirahara[22] considerably different. Discrepancies can, in part, be ascribed to the choice of "base-line" for the transition, since the heat capacity of γ-Cu_2S is about 15 per cent lower than for β-Cu_2S at 355 K. Thus, if β-Cu_2S is used as reference and joined to γ-Cu_2S at 365 K with common molar heat capacity $12.1R$, the transitional enthalpy would be about $36.1R \cdot K$ smaller than reported here. In the determination by Ferrante et al.,[4] a base-line which gives only $3.5R \cdot K$ lower enthalpy than found here, was chosen. The remaining difference of $24.0R \cdot K$ is presumably due to incomplete equilibration of the low-temperature phase in the drop-calorimetric experiment. For the sluggish and composition-dependent $\beta \to \alpha$ transition, a large spread in the values is apparent, and only the results by Jost and Kubaschewski,[23] Kubaschewski,[24] and Ferrante et al.[4] agree reasonably well with ours.

The different kinetic nature of the $\beta \to \alpha$ and $\gamma \to \beta$ transitions is apparent both from the different determinations in the present study and from comparison with the heat-capacity curves of Jost and Kubaschewski[23] and of Kubaschewski[24] for the $\beta \to \alpha$ transition. In their experiments the calorimeter was heated continuously at rates of 0.008 and 0.016 $K \cdot s^{-1}$, and the heat capacity started to rise almost discontinuously at 717 K. In the present experiments with step-wise heating, a considerable rise in heat capacity was observed at 705.82 K for an equilibration time of 35 min, while a rise was already observed at 692.05 K for an equilibration time of 111 min. Thus, the transition proceeds rather slowly, and even after equilibration times of about 20 h, the equilibrium state was not reached. Hence, the present experiments are not quite conclusive as to the question of the $\beta \to \alpha$

TABLE 3. Transformation enthalpies for copper(I) sulfide, Cu_2S
$(R = 8.3144 \text{ J} \cdot \text{K}^{-1} \cdot \text{mol}^{-1})$

γ-Cu_2S to β-Cu_2S		β-Cu_2S to α-Cu_2S		Authors	Year
$\dfrac{\Delta_{trs}H_m}{R \cdot K}$	$\dfrac{T_{trs}}{K}$	$\dfrac{\Delta_{trs}H_m}{R \cdot K}$	$\dfrac{T_{trs}}{K}$		
		$M(Cu_2S) = 159.15 \text{ g} \cdot \text{mol}^{-1}$			
461.9	376	—	—	Bellati and Lussana[19]	1889
451.0	≈ 385	45.7	≈ 720	Ueda[11]	1949
384.9	≈ 385	24.0	≈ 740	Hirahara[22]	1951
—	—	55.3 ± 19.8	710 ± 10	Wehefritz[35]	1960
—	376	144.3 ± 2.41	717	Jost and Kubaschewski[23]	1968
447.4	376	153.9	708 ± 7	Kubaschewski[24]	1973
435.3 ± 3.6	376	141.0 ± 3.6	720	Ferrante et al.[4]	1978
462.7 ± 2.16	376 ± 1	142.8 ± 3.0	710.10	This work	1987

transition being of first or of higher order, but under the conditions of the experiments it behaves as a slow higher-order transition. A typical example is seen in $\Delta_{trs}H_m$ determination C at 718.84 K (table 2) where the energy absorption during the 382 min equilibration time results in a considerably smaller heat capacity than do the adjacent determinations with equilibration times > 1000 min.

Values of the thermodynamic functions derived from the polynomial expressions and of the transformation properties are presented in table 4 for selected temperatures. The accuracy in the thermodynamic functions is estimated to be about 0.3 per cent. Comparison of the derived enthalpies with the drop-calorimetric determinations by Bornemann and Hengstenberg[20] show considerable positive deviation of their results over the common region (9.1 per cent at 573 K and about 1.5 per cent at higher temperatures). A similar, but much less pronounced trend appears in the values by White[21] with a maximum positive deviation of 1.3 per cent at 573 K and a minimum of 0.07 per cent at 873 K. One possible cause for the earlier high values at 573 K is that β-Cu_2S contained some α-Cu_2S before the drops from 573 K by Bornemann and Hengstenberg and traces of α-Cu_2S in the experiments by White. Enthalpy increments relative to 298.15 K obtained subsequent to our determinations by Ferrante et al.[4] are about 1.4 per cent lower for $T = 400$ K and from 0.4 to 0.6 per cent lower for $T = 600$ to 950 K.

TRANSITIONS

The structure of low-chalcocite, γ-Cu_2S, is monoclinic according to Evans[5] with no evidence of any structural disorder, but with strongly anisotropic thermal vibrations for some of the atoms. The approximately hexagonal close-packed S arrangement predicted by Buerger and Buerger[9] was confirmed, and all Cu atoms were found to be triangularly coordinated by S atoms. Above 476 K, the large monoclinic unit cell (48 Cu_2S) transforms into a hexagonal unit cell with only 4 Cu and 2 S atoms. Wuensch and Buerger,[14] Sadanaga et al.,[15] and Cava et al.[16] all discuss the atomic arrangement of β-Cu_2S in terms of the space group P6$_3$/mmc (No. 194).[36] Three non-compatible reflections were noticed, however, by Sadanaga et al.[15] A projection of the structure in the ab-plane is shown in figure 2. According to all proposals the 2 S atoms may be placed in positions 2d (1/3, 2/3, 3/4; 2/3, 1/3, 1/4) and about 1.3 Cu atoms (Cu') are then placed in 2b (0, 0, 1/4; 0, 0, 3/4). These Cu atoms are triangularly coordinated by S at distances $a/3^{1/2} = 229$ pm. In the two earlier proposals, positions 4f (1/3, 2/3, ≈ 0.4; 2/3, 1/3, ≈ 0.9; 2/3, 1/3, ≈ 0.6; 1/3, 2/3, ≈ 0.1) were partially occupied. An occupancy of about 0.4 Cu" per position was suggested by Wuensch and Buerger,[14] and only about 0.1 Cu" by Sadanaga et al.[15] The average occupancy understandably had to be less than 0.5, leaving at most one Cu atom inside each trigonal double pyramid of S atoms.

The remaining 1.1 Cu atoms were placed in positions 6g (1/2, 0, 0; 0, 1/2, 0; 1/2, 1/2, 0; 1/2, 0, 1/2; 0, 1/2, 1/2; 1/2, 1/2, 1/2) in the proposal by Wuensch and Buerger;[14] hence, each of these Cu atoms is linearly coordinated by S. In the proposal by Sadanaga et al.[15] the remaining 2.1 Cu atoms were unequally divided on two 12-fold positions, about 2/3 on one set and 1/3 on the other, with parameters resulting in tetrahedral coordination of the Cu atoms by S.

TABLE 4. Thermodynamic properties of copper(I) sulfide, Cu_2S
$(R = 8.3144 \text{ J} \cdot \text{K}^{-1} \cdot \text{mol}^{-1})$

$\dfrac{T}{K}$	$\dfrac{C_{p,m}}{R}$	$\dfrac{\Delta_0^T S_m^\circ}{R}$	$\dfrac{\Delta_0^T H_m^\circ}{R \cdot K}$	$\dfrac{\Phi_m^\circ(T,0)}{R}$	$\dfrac{T}{K}$	$\dfrac{C_{p,m}}{R}$	$\dfrac{\Delta_0^T S_m^\circ}{R}$	$\dfrac{\Delta_0^T H_m^\circ}{R \cdot K}$	$\dfrac{\Phi_m^\circ(T,0)}{R}$
				$M(Cu_2S) = 159.15 \text{ g} \cdot \text{mol}^{-1}$					
				γ-Cu_2S					
5	0.0195	0.0069	0.0263	0.0016	160	7.540	8.757	727.86	4.2075
10	0.1674	0.0546	0.4113	0.0135	180	7.892	9.666	882.30	4.7641
15	0.4969	0.1799	2.0116	0.0458	200	8.177	10.513	1043.09	5.2972
20	0.9291	0.3805	5.5501	0.1030	220	8.420	11.30	1209.4	5.8086
25	1.4005	0.6382	11.3670	0.1835	240	8.648	12.047	1379.8	6.2969
30	1.8754	0.9357	19.563	0.2836	260	8.867	12.747	1555.0	6.7663
35	2.3287	1.2592	30.086	0.3996	273.15	8.998	13.188	1672.4	7.0650
40	2.7513	1.5981	40.800	0.5281	280	9.063	13.412	1734.3	7.2175
45	3.1410	1.9451	57.541	0.6663	298.15	9.242	13.987	1900.4	7.6121
50	3.4994	2.2948	74.158	0.8116	300	9.262	14.043	1917.5	7.6517
60	4.135	2.9911	112.41	1.1169	310	9.381	14.349	2010.7	7.8627
70	4.687	3.6704	156.58	1.4334	320	9.515	14.649	2105.1	8.0701
80	5.171	4.3285	205.93	1.7544	330	9.656	14.944	2201.0	8.2739
90	5.599	4.9628	259.83	2.0759	340	9.801	15.234	2299.3	8.4745
100	5.976	5.5727	317.73	2.3952	350	10.02	15.521	2397.2	8.6609
120	6.607	6.721	443.83	3.0217	360	10.64	15.810	2499.8	8.8659
140	7.114	7.778	581.20	3.6267	370(γ)	24.1	15.99	2566.6	9.059
				β-Cu_2S					
380(β)	13.2	17.592	3164.7	9.265	560	11.235	22.085	5246.8	12.715
390	11.97	17.891	3279.4	9.481	580	11.166	22.478	5407.7	13.045
400	11.893	18.191	3398.4	9.695	600	11.101	22.854	5693.5	13.366
420	11.806	18.769	3635.3	10.1138	620	11.039	23.218	5914.8	13.677
440	11.719	19.316	3870.6	10.519	640	10.979	23.568	6135.0	13.982
460	11.632	19.835	4104.2	10.914	660	10.920	23.904	6354.0	14.276
480	11.546	20.329	4335.9	11.296	680	10.861	24.229	6571.8	14.565
500	11.463	20.799	4566.0	11.666	700	10.799	24.543	6788.3	14.845
520	11.383	21.246	4794.4	12.026	710(β)	(10.768)	24.696	6896.2	14.982
540	11.307	21.674	5021.4	12.376					
				α-Cu_2S					
710(α)	10.363	24.897	7039.0	14.982	800	9.954	26.103	7948.0	16.168
720	10.276	25.041	7142.2	15.122	850	9.918	26.705	8444.5	16.771
740	10.143	25.321	7346.3	15.394	900	9.923	27.272	8940.4	17.339
760	10.051	25.591	7548.2	15.658	950	9.960	27.810	9437.4	17.875
780	9.991	25.850	7748.6	15.917					

According to the single-crystal neutron-diffraction study of β-Cu_2S by Cava et al.[16] the 6g- and 4f-sites had to be rejected as equilibrium positions for the Cu atoms. The 2.7 Cu atoms (Cu″) were now found to occupy one set of 12k-positions (x, $2x$, z, etc.) with parameters $x \approx 0.26$ and $z \approx 0.43$, resulting in a triangular coordination of S also around Cu″. These Cu″ sites with 0.22 average occupancy are located triangularly around the 4f-positions considered earlier.

Cava et al.[16] studied the structure of β-Cu_2S at 393, 463, 533, and 598 K and found no significant change in the occupancy of the Cu′ 2b- and Cu″ 12k-positions with temperature. This contrasts with the earlier conclusion about increasing electron density at the 2b-positions with temperature in the range 384 to 478 K by
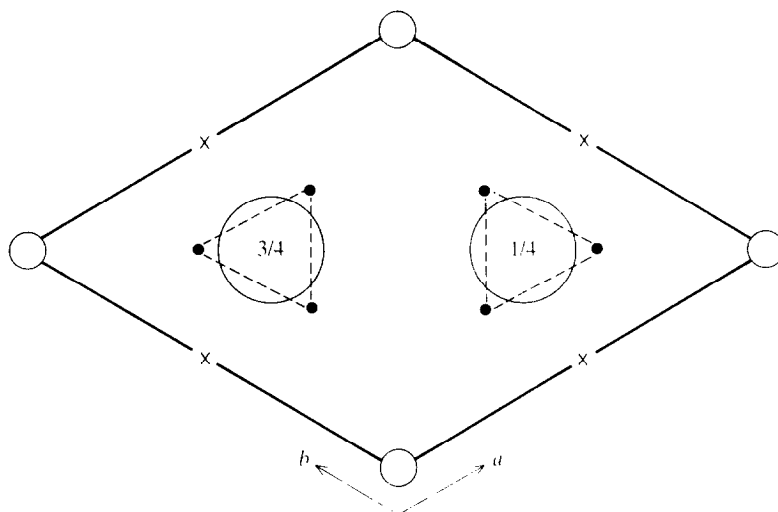
FIGURE 2. Projection of the hexagonal cell for β-Cu_2S in the basal plane (space group P6$_3$/mmc, No. 194). S atoms are in positions 2d (1/3, 2/3, 3/4; 2/3, 1/3, 1/4) and indicated by large circles and the z-parameter. Approximately 1.3 Cu atoms (Cu') are in positions 2b (0, 0, 1/4; 0, 0, 3/4) indicated by small circles. Corners of the left triangle indicate half of the 2.7 Cu" atoms in positions 12k at $z \approx 0.07$ and $z \approx 0.43$, while the other half are at the corners of the right triangle at $z \approx 0.57$ and $z \approx 0.93$. Crosses indicate positions 6g.

Sadanaga et al.[15] Cava et al.[16] saw the relatively high activation energy for Cu transport, 23 kJ·mol^{-1} according to Miyatani and Suzuki[37] and Okamoto and Kawai,[38] as indication of a high potential barrier between the 2b- and 12k-positions.

Above about 710 K the hexagonal structure of β-Cu_2S changes to face-centered cubic. It was originally described by Barth[17] as being of the anti-fluorite type, i.e. a cubic close-packing of S atoms with Cu atoms in all the tetrahedral interstices. Rahlfs[6] examined several possibilities for the structurally related high-digenite, $Cu_{1.80}S$—from that of the ordered anti-fluorite-like type via partially disordered to completely random distribution of 4 Cu atoms over 32 triangular positions— without obtaining satisfactory agreement between observed and calculated X-ray intensities. Morimoto and Kullerud[39] also explored the Cu distribution in high-digenite ($Cu_{1.80}S$) by X-ray precession photographs of natural digenite and found that the intensities were reasonably well explained by random distribution of 7.2 Cu atoms over 192 positions. In a more recent X-ray structural study Gasymov et al.[40] obtained better agreement by assuming a random distribution of the 7.2 Cu atoms over the 8 tetrahedral and 32 triangular positions.

To compare these structural views with the thermodynamic results an estimate of the total transitional entropy from the ordered γ-Cu_2S to the highly disordered β- and α-Cu_2S is needed. For the latter phase, the relatively low and almost constant heat capacity in the range 750 to 950 K indicates practical absence of further positional disorder. As lattice heat-capacity calculations have not yet been carried out for the Cu_2S phases, we have approximated the higher-temperature constant-volume heat capacity by the Debye model with $\Theta_D = 318$ K. It represents the

maximum apparent value for γ-Cu$_2$S after subtraction of the dilation contribution in the 150 K range. The dilational heat capacity can be obtained from the general relation:

$$C_m(d) = C_{p,m} - C_{V,m} = \alpha^2 V_m T/\kappa,$$

where α is the isobaric expansivity, V_m the molar volume, and κ the isothermal compressibility. For γ-Cu$_2$S Ueda[11] reported $\alpha = 208 \times 10^{-6}$ K^{-1}, which apparently is an average value over the range 283 to 373 K. The lattice constant changes from 283 to 323 K—see figure 3 in his paper—correspond to $\alpha \approx 100 \times 10^{-6}$ K^{-1} at 300 K. According to Aliev and Khakimov[41] $\kappa \approx 40 \times 10^{-12}$ Pa^{-1} and the dilational heat capacity is then $C_m(d, 300 \text{ K}) \approx 0.25R$. In the absence of knowledge of the expansivity and compressibility as functions of temperature, the dilational heat capacity may be approximated by the Nernst Lindemann relation:

$$C_m(d) = A(T/T_f)C_{p,m}^2,$$

where A is a general constant and T_f is the melting temperature of the compound (1400 K for Cu$_2$S). Assuming that practically normal expansivity behavior obtains around 900 K we find $A = 0.0019$ J$^{-1} \cdot$ K $\cdot$ mol, which is only 10 per cent higher than ideal (0.00170). The expression approximates the earlier derived $C_m(d, 300 \text{ K})$, and presumably also describes the dilation contribution well for β- and α-Cu$_2$S, just as the Debye-expression with $\Theta_D = 318$ K is expected to describe $C_V(l)$ well above 200 K. The grossly anharmonic vibrations of the Cu atoms present some uncertainty in the derived $C_p(l)$, but are presumably of minor importance compared
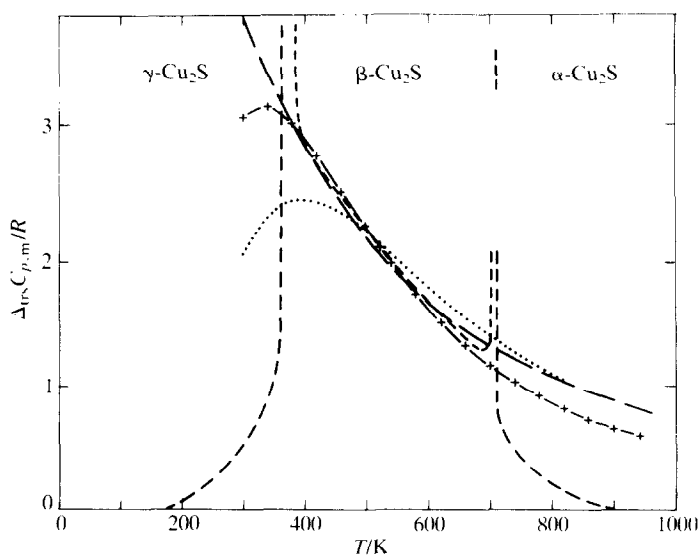

FIGURE 3. Estimated transitional heat capacity of Cu$_2$S. $-\,-\,-$, Present results, $-\,-$, calculated curve for β-Cu$_2$S, fitted to the equation by Schmalzried[30] at 400 and 600 K; $\cdots$, calculated Schkottky heat capacity for $g_0/g_1 = 1/3.8$ and $\Delta E/hc = 820$ cm^{-1} for fit at 500 K; $+ - +$, calculated Schottky heat capacity for $g_0/g_1 = 1/5.7$ and $\Delta E/hc = 740$ cm^{-1} for fit at 500 K.

with the transitional heat capacity in the intermediate temperature range. The anharmonic vibrations seem to influence $C_{V,m}(l)$ in the negative direction, as Ferrante et al.[4] observed a slight decrease in $C_{p,m}$ also above 900 K.

The resulting transitional heat capacity (including its dilational component) is shown in figure 3. A prominent feature is the gradually decreasing $\Delta_{trs}C_{p,m}$ with temperature for β-Cu₂S to that of γ-Cu₂S around 300 K. Thus, the lattice-constant determinations by Cava et al.[16] lead to $\alpha \approx 80 \times 10^{-6}$ K^{-1} as an average value over the range 393 to 598 K, while those by Djurle[12] give $\alpha \approx 110 \times 10^{-6}$ K^{-1}, over the range 425 to 733 K, and Ueda[11] reported $\alpha = 96 \times 10^{-6}$ K^{-1}.

The excess heat capacity of γ-Cu₂S can be analyzed in terms of Frenkel defects among the copper cations by the expression derived by Jost:[42]

$$T^2 \cdot \Delta C_{p,m} = \{\exp(\Delta S_m/2R)\}(\Delta H_m^2/2R) \exp(-\Delta H_m/2RT),$$

by plotting $T^2 \cdot \Delta C_{p,m}$ against $1/T$, see figure 4. The resulting defect formation values are:

$$\Delta_{df}H_m \approx 3.6R \cdot K \quad \text{and} \quad \Delta_{df}S_m \approx 1.6R.$$

The defect formation enthalpy is considerably smaller than the value $\Delta_{df}H_m = 15.6R \cdot K$ derived for γ-Cu₂S (low-chalcocite) by Jost and Kubaschewski,[23] but close to the values we have found[43] for the low-temperature form of Ag₂S: $\Delta_{df}H_m \approx 4.2R \cdot K$ and $\Delta_{df}S_m \approx 1.56R$.

In the thermodynamic approach by Schmalzried[30] the transitional heat capacity is related to physical quantities as compressibility, expansivity, and defect-formation volume, which all need determination at the temperatures in question. Considering also the uncertainty in the presently derived transitional heat capacity—mainly through lack of better founded lattice heat capacity—a detailed analysis is not yet possible for γ-Cu₂S. The decaying heat capacity of β-Cu₂S can, however, be fitted to the equation given by Schmalzried:[30]

$$\Delta C_{p,m} = (R/2)(4T_{max}/T)^2 \exp(-2T_{max}/T) \exp\{-(\Delta_{df}S_m + R \ln z)/2R\},$$

where $\Delta_{df}S_m$ is the molar entropy of defect formation and z the number of equivalent interstitial sites per elementary unit. Correspondence with the
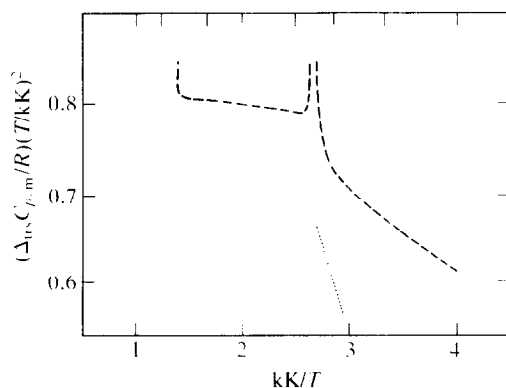

FIGURE 4. Plot of $T^2 \cdot \Delta C_{p,m}$ against $1/T$. – – –, Present results; · · ·, results by Jost and Kubaschewski.[23]

experimental curve at 400 and 600 K leads to $(\Delta_{df} S_m + R \ln z) = 9.80R$ and $T_{max} = 160$ K, see figure 3. Thus, the defect-formation entropy appears to be much larger for β-Cu_2S than for γ-Cu_2S.

According to the structural work by Cava et al.[16] β-Cu_2S is largely disordered, with 1.3 Cu' atoms distributed over 2 equivalent positions and 2.7 Cu" atoms distributed over 12 positions. The maximum molar positional disorder entropy of Cu_2S is then

$$\Delta S_m = -R(0.65 \ln 0.65 + 0.35 \ln 0.35) - 6R(0.225 \ln 0.225 + 0.775 \ln 0.775)$$
$$= (0.65 + 3.15)R = 3.80R.$$

The observed entropy increase in the vicinity of the γ- to β-Cu_2S transition is only a fraction of this, but the transitional entropy increases considerably with temperature for β-Cu_2S. The structural model by Cava et al.[16] does not allow for increased positional disorder for β-Cu_2S with temperature which seems, nevertheless, to be real. The large and decreasing transitional heat capacity in the 400 to 700 K range resembles the tail of a fixed ΔE particle-excitation (Schottky) contribution. In the simplest case, the heat-capacity behavior might be approximated by a Boltzmann excitation of the Cu atoms from a non-degenerate ground level to one with degeneracy leading to the same entropy increment as above:

$$\Delta S_m = 2R \ln \{(g_1 + g_0)/g_0\} = 2R \ln 6.7.$$

If the excitation involves the Cu" atoms only, because of complete randomization of the Cu' atoms at 450 K, one obtains

$$\Delta S_m = 2R \ln 4.8.$$

The corresponding heat-capacity curves, adjusted to the experimental curve at 500 K, are shown in figure 3, where the first alternative and $\Delta E/hc = 740$ cm^{-1} fits remarkably well over the range 380 to 680 K. The related entropy increment, see figure 5, is somewhat smaller than observed in the β-Cu_2S region for the latter alternative, and increasingly larger for the former.

The structure of α-Cu_2S is presumably related to that of high-digenite. Thus, according to the structural picture of $Cu_{1.80}S$ by Morimoto and Kullerud[39] the disorder in stoichiometric α-Cu_2S involves random distribution of 8 Cu atoms on 192 equivalent positions. Without restrictions about occupation of neighboring lattice sites, the positional entropy increment is unreasonably large $(23.6R)$ both absolutely, and relative to that of β-Cu_2S.

The structural model by Gasymov et al.[40] for $Cu_{1.80}S$ leads, when applied to α-Cu_2S, to an entropy increment closer to that observed. Thus, with 4 Cu atoms in an 8-fold position and 4 Cu" atoms in a 32-fold position, the molar positional entropy increment for Cu_2S would be

$$\Delta S_m = -2R(0.5 \ln 0.5 + 0.5 \ln 0.5) - 8R(0.125 \ln 0.125 + 0.875 \ln 0.875)$$
$$= (1.39 + 3.01)R = 4.40R.$$

It is surprising that the different nature of the Cu atoms should persist above the β- to α-Cu_2S transition at 710 K. We would rather assume that this difference
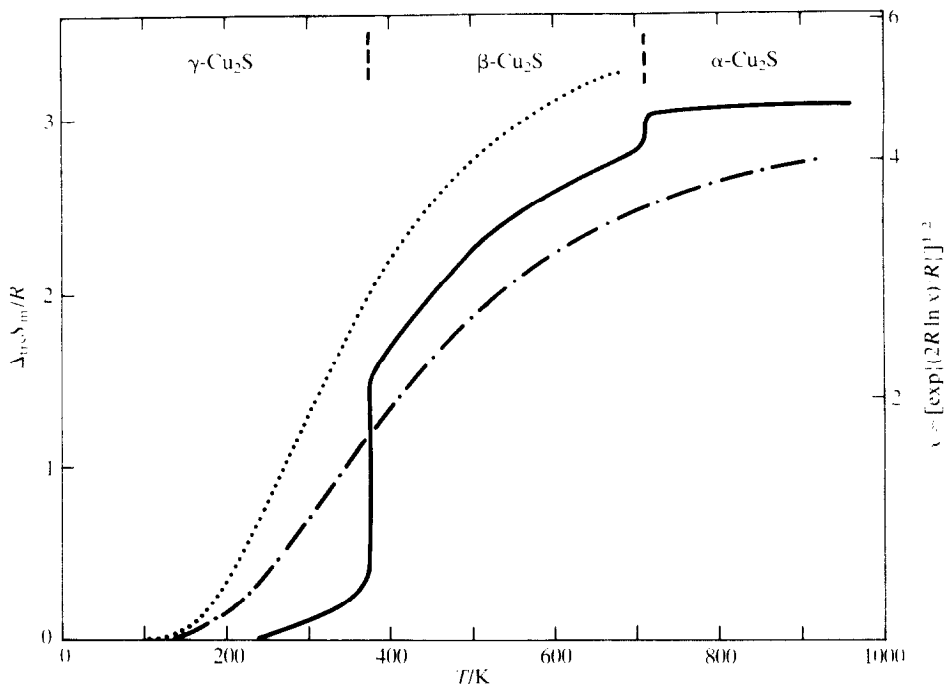
FIGURE 5. Transitional entropy of Cu_2S. ——, Present experimental results; —●—, entropy acquired in a Schottky-type transition with $g_0/g_1 = 1/3.8$ and $\Delta E/hc = 920$ cm^{-1}; · · ·, entropy acquired in a Schottky-type transition with $g_0/g_1 = 1/5.7$ and $\Delta E/hc = 740$ cm^{-1}.

disappears at 710 K and that no appreciable further positional disorder occurs before melting is approached. The β- and α-Cu_2S transition might thus imply equivalence between the 1.3 Cu' and the 2.7 Cu" atoms in the model by Cava et al.[16] for β-Cu_2S, i.e.:

$$\Delta S_m = -7R(0.2857 \ln 0.2857 + 0.7143 \ln 0.7143) - 3.80R = 0.38R.$$

The experimental transitional entropy at 710 K is comparable (0.20R) with that for the last alternative, assuming that only slight changes in the bonding properties occur simultaneously. In this connection it should be noted that the low driving force and kinetic factors result in the formation of intermediate structures. High-temperature X-ray diffraction results by Dubrovina et al.[44,45] show that 12H and 14H polytypes arise as a result of periodically distributed stacking faults in the hexagonal to cubic lose-packing of the sulfur atoms. With heating rates of 5.5 mK · s^{-1} the transition range extended from 700 to 750 K.

REFERENCES

1. Anderson, C. T. *J. Am. Chem. Soc.* **1932**, 54, 107.
2. Mills, D. C. *Thermodynamic Data for Inorganic Sulphides, Selenides, and Tellurides.* Butterworths: London. **1974.**
3. Potter, R. W., II. *Econ. Geol.* **1977**, 72, 1524.
4. Ferrante, M. J.; Stuve, J. M.; Daut, G. E.; Pankratz, L. B. *Bur. Mines (U.S.) Rept. Investig. 8305,* **1978**; see also *High-Temp. Sci.* **1981**, 14, 77.
5. Evans, H. T., Jr. *Nature, Phys. Sci.* **1971**, 232, 69.
6. Alsén, N. *Geol. Fören. Forh.* **1931**, 53, 111.
7. Rahlfs, P. *Z. Phys. Chem. B* **1936**, 31, 157.
8. Buerger, N. W. *Econ. Geol.* **1941**, 36, 19.
9. Buerger, M. J.; Buerger, N. W. *Am. Mineral.* **1944**, 29, 55.
10. Oftedal, I. *Norsk Geol. Tidskr.* **1945**, 24, 114.
11. Ueda, R. *J. Phys. Soc. Jpn* **1949**, 4, 287.
12. Djurle, S. *Acta Chem. Scand.* **1958**, 12, 1415.
13. Belov, N. V.; Butuzov, V. P. *Dokl. Akad. Nauk S.S.S.R.* **1946**, 54, 717.
14. Wuensch, B. J.; Buerger, M. J. *Mineral. Soc. Am. Spec. Paper* **1963**, 1, 164; see also Buerger, M. J.; Wuensch, B. J. *Science* **1963**, 141, 276.
15. Sadanaga, R.; Ohmasa, M.; Morimoto, N. *Mineral. J. Jpn* **1965**, 4, 275.
16. Cava, R. J.; Reidinger, F.; Wuensch, B. J. *Solid State Ionics* **1981**, 5, 501.
17. Barth, T. *Zentralbl. Mineral. Geol. Paläont. A* **1926**, 284.
18. Roseboom, E. H., Jr. *Econ. Geol.* **1966**, 61, 641.
19. Bellati, M.; Lussana, S. *Atti. Ist. Veneto* **1889**, 7, 1051.
20. Bornemann, K.; Hengstenberg, O. *Metall u. Erz* **1920**, 17, 313.
21. White, W. P. *J. Am. Chem. Soc.* **1933**, 55, 1047.
22. Hirahara, E. *J. Phys. Soc. Jpn* **1951**, 6, 422; see also *ibid.* **1947**, 2, 211.
23. Jost, W.; Kubaschewski, P. *Z. Phys. Chem. N.F.* **1968**, 60, 69; see also *Nachr. Akad. Wissensch. Göttingen, Math. Phys. Kl.* **1968**, No. 2.
24. Kubaschewski, P. *Ber. Bunsen-gesellschaft Phys. Chem.* **1973**, 77, 74.
25. Grønvold, F.; Kveseth, N. J.; Marques, F. D. S.; Tichy, J. *J. Chem. Thermodynamics* **1972**, 4, 795.
26. Grønvold, F.; Sveen, A. *J. Chem. Thermodynamics* **1974**, 6, 859.
27. Jost, W.; Oel, H. J.; Schniedermann, G. *Z. physik Chem. N.F.* **1958**, 17, 175.
28. Nölting, J.; Rein, D.; Troe, J. *Nachr. Akad. Wissensch. Göttingen, Math. Phys. Kl.* **1969**, No. 4.
29. Kubaschewski, P.; Nölting, J. *Ber. Bunsen-gesellschaft Phys. Chem.* **1973**, 77, 70.
30. Schmalzried, H. *Ber. Bunsen-gesellschaft Phys. Chem.* **1980**, 84, 120.
31. Hambling, P. G. *Acta Cryst.* **1953**, 6, 98.
32. Potter, R. W., II; Evans, H. T., Jr. *J. Res. U.S. Geol. Surv.* **1976**, 4, 205.
33. Westrum, E. F., Jr.; Furukawa, G. T.; McCullough, J. P. *Experimental Thermodynamics, Vol. I.* McCullough, J. P.; Scott, D. W.: editors. Butterworths: London. **1968**, p. 133.
34. Grønvold, F. *Acta Chem. Scand.* **1967**, 21, 1695.
35. Wehefritz, V. *Z. Phys. Chem.* **1960**, 26, 339.
36. *International Tables for Crystallography. Vol. A.* Hahn, T.: editor. Reidel Publ. Co.: Dortrecht/Boston. **1983.**
37. Miyatani, S.; Suzuki, Y. *J. Phys. Soc. Jpn* **1953**, 8, 630.
38. Okamoto, K.; Kawai, S. *Jap. J. Appl. Phys.* **1973**, 12, 1130.
39. Morimoto, N.; Kullerud, G. *Am. Mineral.* **1963**, 48, 110.
40. Gasymov, G. B.; Asadov, Yu. G.; Guseinov, G. G.; Belov, N. V. *Dokl. Akad. Nauk S.S.S.R.* **1978**, 239, 846; see also *Soviet Phys. Dokl.* **1978**, 23, 218.
41. Aliev, F. Yu.; Khakimov, K. *Dokl. Akad. Nauk Tadzh. S.S.R.* **1978**, 21, 31.
42. Jost, W. *Diffusion in Solids, Liquids and Gases.* Academic Press: New York. **1960**, p. 95.
43. Grønvold, F.; Westrum, E. F., Jr. *J. Chem. Thermodynamics* **1986**, 18, 381.
44. Dubrovina, A. N.; Gorelik, S. S.; Plyusnin, A. B.; Reznitskii, M. E.; Ukrainskii, M. Yu. *Izv. Vyssh. Uchebn. Zaver, Fiz.* **1976**, 19, 626.
45. Plyusnin, A. B.; Dubrovina, A. N.; Finarev, M. S. *Soviet Phys. Crystallogr.* **1978**, 23, 476; *ibid.* **1979**, 24, 344.